CHANG CHEN
SHIFU ZHANG
SHIQIANG SONG
QIXIN ZHANG
JIKUN GUO
and
BINBIN YU

Finite element analysis on deformation and stress distributions of double-wall oil tank under double supports installation mode

The double-wall oil tank is more and more widely used in filling station due to the characteristics of corrosion protection, safety and economy. However, the outer tank of SF double oil tank has thinner wall thickness and lower strength, improper installation method may cause damage to the tank. In this paper, a simplified finite element model of double tank is established according to the structural characteristics of SF double-wall oil tank. Focusing on the 20 m^3, 30 m^3 and 50 m^3 oil tanks which are widely used in the current gas stations, the deformation and stress distribution of the oil tanks under different bearing width and support position are calculated by ANSYS software respectively. Taking the 30 m^3 oil tank as an example, the deformation, stress distribution characteristics and the influence of the bearing support position on the stress distribution are analyzed in detail, which would provide guidance for selecting the reasonable size and position of supporting bearing under double supports installation mode.

Keywords: *Numerical simulation, stress distribution, double-wall oil tank, double supports installation mode.*

1. Introdunction

SF double-wall oil tank is called steel reinforced glass fiber double tank, also known as jacketed tank adopting double structure of the glass fiber reinforced plastic outer tank and steel inner tank. The double tank is equipped with leakage detection device, which can realize the function of 24h on-line monitoring and leakage automatic alarm. What is more, it has the characteristics of corrosion protection, safety and economy. Since the outer tank of SF double oil tank has thinner wall thickness and lower strength, improper installation method may cause damage to the outer tank. During the installation and usage of underground oil tank, the peak stress of the tank will change with the change of depth of burial, actual volume of liquid storage, bearing size and supporting position of bearing. In the case where the oil tank is buried at a certain depth, the supporting position and the size of bearing have the most significant influence on the peak stress of oil tank. Considerable research efforts have been devoted to this area. Bridges, T. F analyzed the features of double-wall tank for LNG, and pointed out that either 5083-0 aluminum alloy or 9% nickel steel being suitable for LNG containment at a service temperature of - 260 F (Bridges, 1971). Kaempen, Charles E described how a double wall filament wound glass fiber reinforced plastic underground storage tank (UST) can be stiffened by a non-removable steel frame mandrel that remains within the tank (Kaempen, 1996). Arao, M proposed a generic concept of 'Flexible Intelligence Machine Control (FIMC)' which has a hierarchical structure and two functions of knowledge acquisition and adaptive learning, and shown a practical example of FIMC which is applied to a temperature control on the actual jacket tank in polymerization process (Arao, et al., 1998). Wu, Yun-Long introduced the structure, material, fabrication, inspection and insulation for large welded steel double wall refrigerated tank (Wu, et al., 2002). Mjalli, F. S. presented a novel steady-state design algorithm to stabilize the CSTR by replacing the single CSTR by a cascade of reactors that are capable of stabilizing and maintaining the unstable steady state (Mjalli and Jayakumar, 2009). Wilkowski, Gery conducted a detailed investigation about the fractured failure of the heads on both the outer carbon steel and the inner aluminum vessel of liquid nitrogen (LN2) storage tank (Wilkowski, et al., 2010). Aimikhe, V. J. developed a model for predicting internal tank diameters that will yield minimum boil off gas production in LNG above ground double wall metallic storage tanks (Aimikhe, 2011). Jeong, Jae-Hyun carried out the evaluation of the insulation effect by the thermal conductivity of perlite powder and the effect of heat flux by welding conditions with insulation analysis of double-wall and performed thermal and structural analysis of the tank to study the effect of vacuum and weldment geometry of the internal supports (Jeong, et al.,

Messrs. Chang Chen, Shifu Zhang, Qixin Zhang, Jikun Guo, Army Logistics University of PLA, Chong Qing, 401311, Shiqiang Song, Logistics Training Center of PLA Rocket Force, Hebei 075000 and Binbin Yu, Navy Logistics University of PLA, Handan 056000, China. Corresponding author Chang Chen, E-mail: 408430734@qq.com

2013). Li, Yipeng researched the difficulty of the static electricity in the fiber reinforced plastics (FRP) double wall underground storage gasoline tanks to decay into the earth (Li, et al., 2013). Y Liu built up the finite element model of FRP buried double-wall tank by using the ABAQUS/CAE module to analyze the reliability and applicability of FRP buried double-wall tank on filling station construction (Liu, et al., 2015). Yang, Jinlin introduced the performance, category and structure of horizontal double deck oil tanks, and combined with the successful promotion experience in technology developed countries to outlook the wide application prospects of double deck oil tanks in China due to its advantages in the aspects of safety, environmental protection and economic practicality (Yang, et al., 2016).

In this paper, the installation method of underground oil tank and the distribution of soil pressure outside the tank are analyzed. According to the structural characteristics of SF double-wall oil tank, a simplified finite element model of double tank is established, and the deformation and stress distribution of the oil tanks under different bearing width and support position are calculated by ANSYS software respectively, which would provide guidance for selecting the reasonable size and position of supporting bearing.

Following the introduction, the rest of this paper is organized as follows. Section 2 analyzes the installation method of underground oil tank. Section 3 analyzes the load of underground SF double-wall tank. Section 4 establish the finite element model of double-wall oil tank. Section 5 analyzes the deformation, stress distribution characteristics and the influence of the bearing support position on the stress distribution. Section 6 concludes the paper.

2. Installation method of underground oil tank

Due to the improvement of environmental protection requirements in urban areas, the installation methods of underground oil tanks have changed a lot compared to the past. The usual method is to install the underground tank in an impervious pond constructed of impervious concrete (technical code for prevent leakage of underground storage tank, 2008). Generally, 2 saddle shaped concrete bearings are arranged in the anti-seepage pool, and the support and the anti-floating belt wrapped on the outer surface of the oil tank are fixed by setting the anchor bolt, thereby connecting the oil tank with the bearing as a whole. After the tank is fixed in the anti-seepage pond, the remaining space in the pond is filled with neutral fine sand and coarse sand in turn. The top of the impervious pond is paved with concrete and impervious measures are adopted to prevent the leakage of oil from the outside, and rainwater penetrates into the seepage prevention pond. Compared to the traditional single-layer steel tank, the environmental performance of SF double tank is greatly improved, so it is not necessary to build an impermeable pool. Only the concrete foundation is needed, and the saddle shaped concrete support and the anti-floating strap shall be installed accordingly. In order to prevent the concrete support and the anti-floating holding band from damaging the glass steel outer tank, a rubber pad is arranged correspondingly to the contact part of the outer tank (code for design of oil depot, 2014). This paper focuses on deformation and stress distributions of double-wall oil tank under double supports installation mode.

3. Load analysis

The load of the underground tank includes the gravity of tank, the gravity of medium in tank and the soil pressure outside the tank, besides the accidental load on the ground. Because the gravity of tank and the gravity of medium in tank are related to oil tank, this paper mainly analyzes soil pressure outside the tank and the accidental load on the ground.

3.1 Soil pressure outside the tank

In engineering design, it is generally considered that soil is a continuum composed of soil particles, water and gas. Continuum mechanics is used to study the distribution of pressure in soil and to calculate the pressure on the unit area of soil (Song, 2002). The soil pressure acting on the outer surface of the tank is produced by the combined action of the vertical soil pressure and the lateral soil pressure σ_{cx}. As shown in Fig.1, a point is taken at the outer surface of the tank at depth H, and the vertical soil pressure acting on that point is

$$\sigma_{CH} = \rho Hg$$

$$H = H_0 + R_0 (1–\sin \theta) \quad (1)$$

In formula (1), ρ represent the soil density, and ρ=1400~1650 kg/m^3 for dry fine sand, ρ=1400~1800 kg/m^3 for dry coarse sand, ρ=1800~2400 kg/m^3 for concrete. H represents the distance of this special point from the outside surface of the tank to the ground. H_0 represents the distance from top of double-wall tank to the ground represents the outer diameter of double-wall tank. g = 9.81 m/s^2.

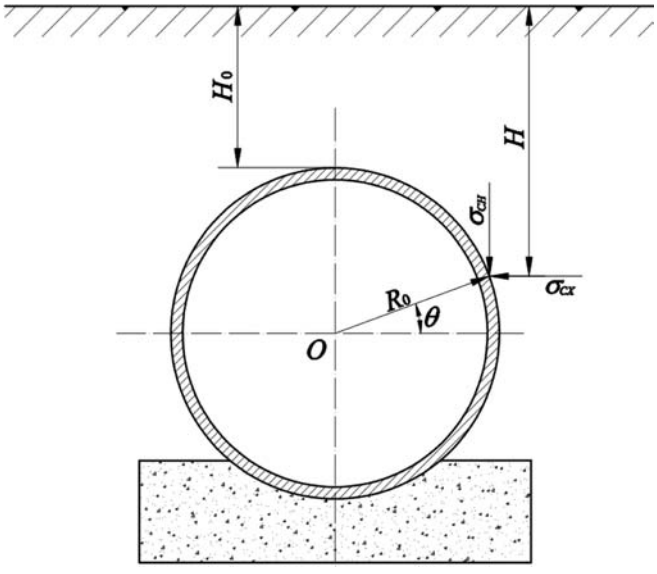

Fig.1. Analysis of soil pressure at depth H

Assuming that the ground is an infinite horizontal plane, the vertical soil pressure is evenly distributed along any horizontal plane, so the soil can only produce vertical deformation under its own gravity without lateral deformation and shear deformation. From this point of view, according to the theory of elasticity, it can be considered that the lateral soil pressure acting on the outer surface of the tank should be proportional to the vertical soil pressure and the shear force is zero.

$$\sigma_{CX} = K_0\sigma_{CH} \quad (2)$$

In formula (2), K_0 represents lateral pressure coefficient of soil, and K_0 = 0.18~0.25 for gravel soil, K_0 = 0.25~0.33 for sandy and stony soil, K_0 = 0.33~0.42 for clay soil.

As shown in Fig.2, the element at outer surface of the tank is regarded as the research object, the center angle corresponding to the infinitesimal equals θ, the length of the element equals dl, the infinitesimal is approximated as the beveled edge of a triangular element and the normal pressure on the bevel is regarded as the soil pressure of outer surface element of oil tank (Zhou, et al., 2007).

$$pdl = \sigma_{CH}dl\ \sin\theta\ \sin\theta + \sigma_{CX}\ dl\ \cos\theta\ \cos\theta \quad (3)$$

$$\begin{aligned} p &= \sigma_{CH}\ \sin^2\theta + \sigma_{CX}\ \cos^2\theta \\ &= \sigma_{CH}\ (\sin^2\theta + K_0\ \cos^2\theta) \\ &= \sigma_{CH}\ [1-(1-K_0)\ \cos^2\theta] \end{aligned} \quad (4)$$

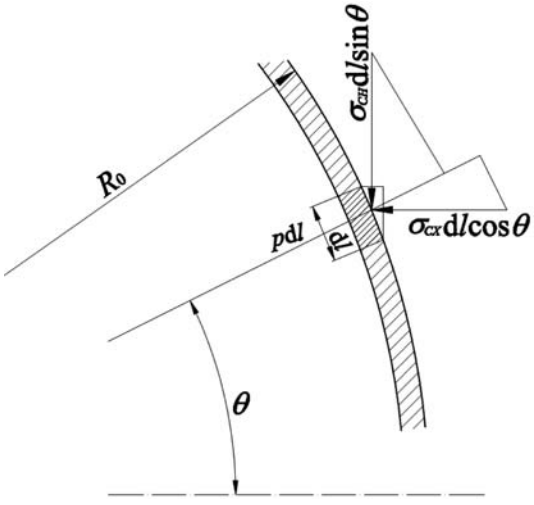

Fig.2. Force analysis diagram of infinitesimal

Comprehensive consideration of equation (1) and equation (4), the functional relation of the soil pressure with the change of the center angle can be simplified to obtain as follow.

$$p = \rho g[H_0 + R_0\ (1-\sin\theta)]\ [1-(1-K_0)\ \cos^2\theta] \quad (5)$$

Fig.3 shows the distribution regulation of soil pressure on the outside surface of the tank. It can be seen from the figure that the maximum soil pressure outside the tank occurs at the top of the tank, $\theta = 90^o$.

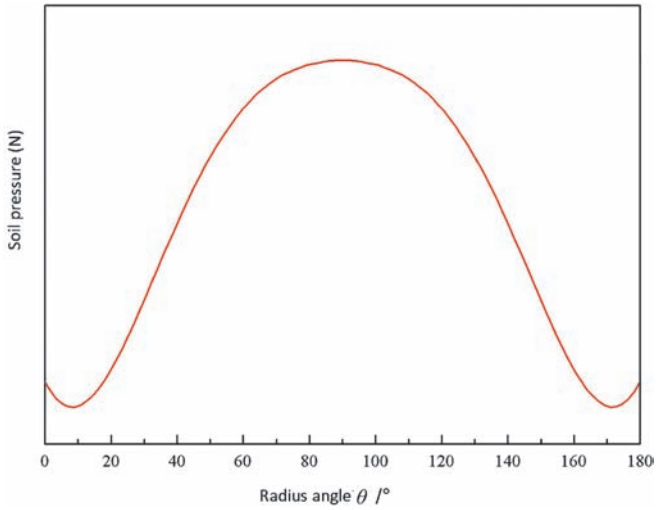

Fig.3. Distribution diagram of soil pressure

3.2 Other accidental loads

Accidental load is the temporary load on the ground, such as the temporary vehicle passing on the ground. Accidental loads generally do not need to be calculated separately. If accidental loads are taken into account during the calculation, multiplied coefficients 1.5~2.0 are added on the basis of soil pressure (He, et al., 2007).

4. Establishment of finite element model of double-wall oil tank

Taking the 20 m^3, 30 m^3 and 50 m^3 oil tanks which are widely used in the current gas stations as examples, the deformation and stress distribution of the oil tanks in different bearing widths and supporting positions are calculated respectively.

4.1 Model assumptions and simplification

According to the structure and stress condition of SF double-wall tank, the structure mechanics are used to simplify the actual structure, and the local structure such as vertical pipe and manhole are neglected. In fact, double-wall oil tank can be considered as a composite structure composed of three layers of different materials, such as outer tank, middle layer and inner tank. FRP outer tanks are sprayed with a mixture of resin and short fibers to form an overall shape. The short fibers are basically two-dimensional and randomly distributed in the resin (Yang, 2000), so they can be assumed to be isotropic. The middle layer is formed by painting the plastic particles on the outer surface of the inner tank (Wang and Gao, 2012). Since both the space between the plastic particles and the thickness of the middle layer are small, it is reasonable to assume the middle layer to be an isotropic material in the calculation.

4.2 Establishment of geometric model

(1) The structure and size of the computational model

In this paper, the SF double-wall tank used in the oil-gas station is taken as the research object. The tank is mounted

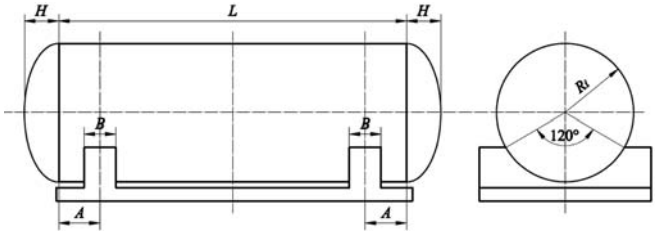

Fig.4. Installation diagram of oil tank

TABLE 1 GEOMETRIC DIMENSIONING OF SOLID MODEL

Tank volume	Parameter	Value
20 m^3	Cylinder length L/mm	5770
	Cylinder diameter D/mm	2000
	wall thickness of inner tank δ_1/mm	6
	middle layer thickness δ_2/mm	0.2
	wall thickness of outer tank δ_3/mm	4
	Ellipsoid height H/mm	500
30 m^3	Cylinder length L/mm	5880
	Cylinder diameter D/mm	2400
	wall thickness of inner tank δ_1/mm	6
	middle layer thickness δ_2/mm	0.2
	wall thickness of outer tank δ_3/mm	4
	Ellipsoid height H/mm	600
50 m^3	Cylinder length L/mm	7300
	Cylinder diameter D/mm	2800
	wall thickness of inner tank δ_1/mm	8
	middle layer thickness δ_2/mm	0.2
	wall thickness of outer tank δ_3/mm	4
	Ellipsoid height H/mm	700

with two supports and the supporting angle is 120 degrees. Fig.4 shows the installation illustration of the double-wall tank, and the main geometric dimensions of the tank are shown in Table 1.

(2) Mechanical properties of components

Mechanical properties of the components of SF double-wall oil tank are shown in Table 2.

(3) Construction method of finite element model

For the composite structure, the modelling method mainly includes the separation model, the modular model and the integral model (Tan, 2002). The integral modelling method is simple in modelling process and low in computational complexity, but it cannot reveal the mechanism of interaction between the layers and the stress distribution of each layer. Therefore, this paper adopts the separate modelling method to model the outer tank, middle layer and inner tank separately. And then the three parts are integrated as a whole to study the stress distribution of double-wall oil.

4.3 ESTABLISHMENT OF COMPUTATIONAL MODEL

In order to analyze the influence of bearing support position and bearing size on the structural strength of SF double tank, a series of models were established with the bearing support position and bearing size as variables. Considering that the structural dimensions of the double-wall tank under different volumes are not the same, the position parameter is introduced when defining the support position. The specific calculation model is shown in Table 3. As the calculation model of the double-wall tank is symmetrical in terms of load and structure, in order to reduce the calculation load, only one quarter of the model is calculated in the calculation. Fig.5 shows the 1/4 entity simplified model during the ANSYS calculation.

4.4 MESH PARTITION

In the mesh partition process, the three-dimensional 8-node SOLID185 unit is selected for meshing the main structure of double-wall tank, and SOLID65 unit is selected for meshing the bearing. In order to improve the accuracy of the calculation, the grid is all hexahedral element. The non-linear contact algorithm is used to support the interface between the bearing and the tank, and the three-dimensional surface-contact elements TARGE170 and CONTA174 are adopted. The normal stiffness coefficient of the contact surface is defined as 0.1. Fig.6 shows the mesh generation result of the model.

TABLE 2. MATERIAL MECHANICAL PROPERTIES FOR S&F DOUBLE-WALL OIL TANK

Components	Material	Parameter	Value
Outer tank	glass fiber	Elastic modulus E/MPa	0.724×105
		density ρ/kg/m^3	1.85×103
		Poisson ratio μ	0.34
Middle layer	polyvinyl chloride	Elastic modulus E/MPa	3.5×103
		density ρ/kg/m^3	1.4×103
		Poisson ratio μ	0.35×103
Inner tank	carbon steel	Elastic modulus E/MPa	2.06×105
		density ρ/kg/m^3	7.86×103
		Poisson ratio μ	0.3
Support	concrete	Elastic modulus E/MPa	22.1×103
		density ρ/kg/m^3	2.0×103
		Poisson ratio μ	0.15

TABLE 3 LOCATION PARAMETER DEFINITION

Bearing width B/mm	Support position A/L									
200	0.04	0.06	0.08	0.10	0.12	0.14	0.16	0.18	0.20	0.22
400	0.04	0.06	0.08	0.10	0.12	0.14	0.16	0.18	0.20	0.22
600	–	0.06	0.08	0.10	0.12	0.14	0.16	0.18	0.20	0.22

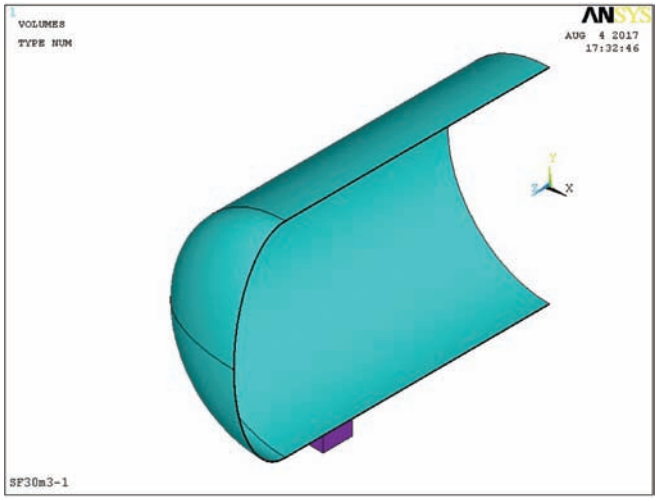

Fig.5. 1/4 solid simplified model

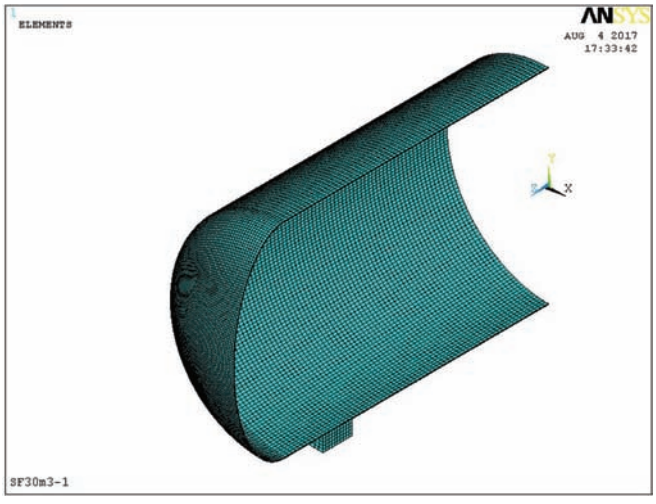

Fig.6. Finite mesh generation

4.5 BOUNDARY CONDITION SETTING

Because when the double-wall tank is fulfilled with oil, the tank would face higher security risk. Therefore, the tank under fulfilling load is taken as research object in this paper. The constraint of the base of the support is a fixed constraint. The constraint on the symmetry surface is symmetric constraint, that is, there is no displacement or rotation angle in the direction perpendicular to the symmetry surface, and the shear force on the symmetric plane is zero.

4.6 LOAD CONDITION SETTING

According to the (code for design and construction of filling station) (GB50156-2012), the soil thickness above the tank top should not be less than 0.5 m when the tank is buried below the non-roadway. When the tank is buried below the roadway, the soil thickness above the tank top shall not be less than 0.9 m (code for design and construction of filling station, 2012). In this paper, it is assumed that the soil thickness above the double-wall oil tank is 900 mm, which is filled with dry fine sand and dry coarse sand. And the ground is paved with concrete. Their thicknesses are 300 mm, 450 mm, 150 mm respectively. Besides, the accidental load factor equals 2. In order to simplify the calculation, the supporting role of the soil below the double-wall tank is neglected, and it is considered that the load on the double-wall tank is all borne by the support.

5. Results and analysis

Three different specifications of SF double-wall oil tank are calculated in each model, so as to analyse the deformation and stress distribution regulation of oil tank during installation and use process.

5.1 ANALYSIS OF OIL TANK DEFORMATION

Table 4 shows the maximum deformation of oil tank with different model parameter, and it can be seen that the maximum deformation of the tank increases with the increase of the supporting position A/L, and the maximum deformation decreases with the increase of the bearing width B. What is more, the maximum deformation of the tank increases with the increase of the tank volume.

Taking the model of the double-wall oil tank with the capacity of 30, the supporting position A/L=0.10 and the bearing width B=400 mm as an example, the deformation distribution of oil tank are shown in Fig.7(a). It can be seen from the figure that the deformation of the double-wall oil tank near the ellipsoid part is very small due to the restraint effect of the ellipsoid part on the main body of the tank. The closer to the middle section of the oil tank, the flat deformation of the tank is more obvious due to the effects of medium in the tank, the tank weight and the soil pressure outside the tank.

Fig.7(b) shows the deformation of intermediate section of oil tank, and Fig.7(c) shows the deformation of middle bearing section. It can be seen from the figure that the curvature at intermediate section of oil tank change gently. As the stiffness of bearing is larger than the rigidity of tank, the oil tank deformation at the middle section of the bearing is limited, resulting in almost no deformation of the tank at the contact part with the bearing, while the curvature of the tank at the corner of the bearing is greatly changed. Fig.7(d)

TABLE 4. MAXIMUM DEFORMATION OF OIL TANK WITH DIFFERENT MODEL PARAMETER (UNIT: MM)

A/L	B=200 mm			B=400 mm			B=600 mm		
	20 m^3	30 m^3	50 m^3	20 m^3	30 m^3	50 m^3	20 m^3	30 m^3	50 m^3
0.04	2.49028	3.11566	3.87502	2.19477	2.60811	3.48888	-	-	-
0.06	2.68442	3.12103	4.13705	2.40199	2.81010	3.76829	2.13990	2.56314	3.47192
0.08	2.84760	3.31674	4.40665	2.59043	3.00962	4.02441	2.33151	2.73513	3.72265
0.10	3.02469	3.47317	4.58726	2.73115	3.21095	4.21099	2.48237	2.93667	3.97484
0.12	3.13502	3.68224	4.86369	2.92156	3.36118	4.47050	2.67024	3.10013	4.16123
0.14	3.42290	3.88339	5.13034	3.16806	3.55871	4.66199	2.99708	3.30812	4.41372
0.16	3.75944	4.05681	5.33367	3.49820	3.71794	4.89665	3.27334	3.51636	4.64702
0.18	4.05478	4.27053	5.63830	3.82153	3.95086	5.23871	3.59472	3.73210	4.97096
0.20	4.37634	4.45417	5.87059	4.09578	4.22073	5.53593	3.87572	3.99301	5.32606
0.22	4.68919	4.73916	6.25653	4.40188	4.44136	5.89599	4.18009	4.22319	5.59925

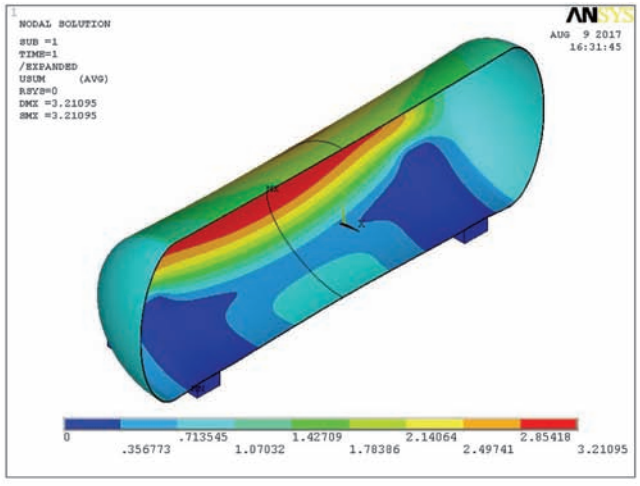

(a) Deformation distribution of oil tank

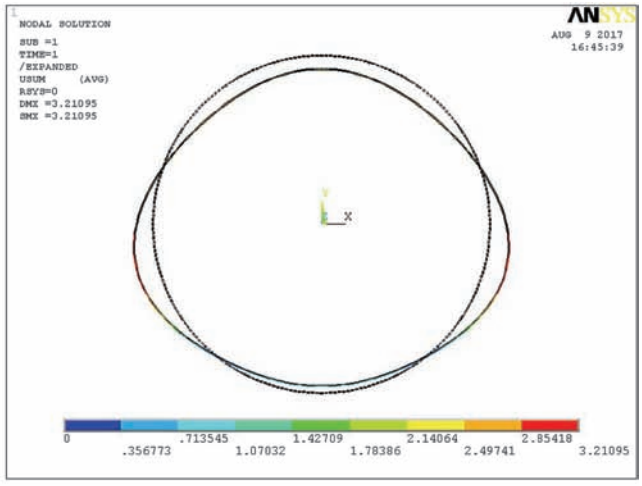

(b) Deformation of intermediate section of oil tank

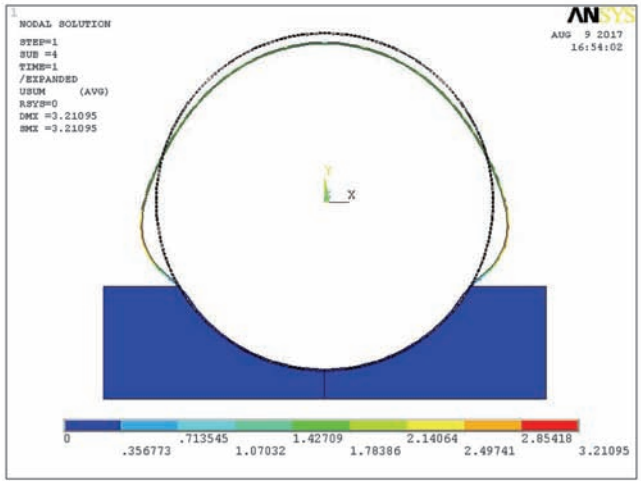

(c) The deformation of middle bearing section

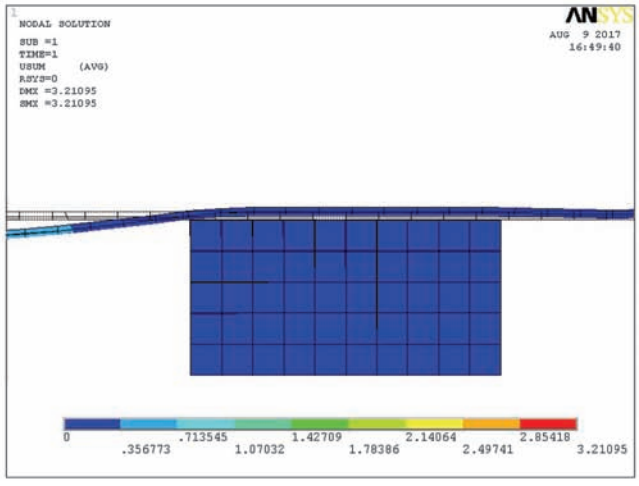

(d) the amplify deformation at supporting position

Fig.7. Deformation diagram of tank

shows the deformation of the tank at the bearing position. It can be seen that the deformation of the tank is larger than that of the bearing, resulting in a closer contact between the tank and the bearing in the outside of the bearing, while a separation trend between the tank and the bearing in the inside of the bearing, which also causes a large stress concentration area to occur on the outside of the tank.

Table 5. Maximum equivalent stress of outer tank with different parameter (unit: MPa)

A/L	B=200 mm			B=400 mm			B=600 mm		
	20 m^3	30 m^3	50 m^3	20 m^3	30 m^3	50 m^3	20 m^3	30 m^3	50 m^3
0.04	37.1193	47.2473	48.9513	30.0359	32.7087	37.3913	-	-	-
0.06	41.1576	47.9957	53.3383	34.3913	35.3061	41.6407	28.1334	30.6398	35.0580
0.08	48.4069	51.5385	60.1880	37.0313	37.6306	43.6589	31.2946	32.8662	37.5638
0.10	51.6805	53.1995	59.0843	38.2233	42.7383	45.2538	32.9533	34.7380	42.6142
0.12	55.9473	54.9752	70.2183	43.0278	43.8791	51.8398	34.3273	35.4045	43.7045
0.14	54.0886	57.3799	68.2522	43.9771	45.5882	52.6447	35.3025	38.9301	45.5087
0.16	56.0165	63.0518	71.0154	45.3195	47.8969	51.7603	38.1486	39.969	45.1874
0.18	62.9697	65.1876	77.8465	45.8141	46.5066	55.3588	38.9505	39.9615	46.3621
0.20	64.7579	65.4061	72.8806	45.7761	51.2894	55.3268	39.0938	39.9487	50.9081
0.22	66.3337	66.6562	84.3318	50.5333	51.2249	61.5449	41.4457	40.5393	50.3069

Table 6. Maximum equivalent stress of middle layer with different parameter (unit: MPa)

A/L	B=200 mm			B=400 mm			B=600 mm		
	20 m^3	30 m^3	50 m^3	20 m^3	30 m^3	50 m^3	20 m^3	30 m^3	50 m^3
0.04	4.41501	12.0188	7.17295	6.60849	6.82432	7.56495	-	-	-
0.06	4.45140	7.87731	7.48709	6.77283	6.09257	7.77367	6.58991	7.08331	6.24082
0.08	7.59016	8.02779	7.02629	6.35235	6.52387	7.16430	6.59285	6.87447	6.57228
0.10	7.99503	8.08388	5.86989	4.75790	7.47622	4.83801	6.33901	4.42360	7.64774
0.12	13.0059	6.87875	11.1122	7.75656	7.37815	8.67786	6.20635	6.56678	7.45405
0.14	6.24105	7.52101	14.3466	7.55075	7.16970	8.70286	6.54515	6.96648	7.23173
0.16	6.11646	9.90171	10.8884	7.14281	12.5681	5.34953	6.54524	6.96053	6.63380
0.18	10.2076	10.1768	10.9492	7.37800	6.74245	8.18593	6.33733	6.44696	6.82749
0.20	10.2203	10.2314	7.21148	4.89834	8.42613	5.58467	6.65613	4.52232	8.80472
0.22	9.73743	9.61014	13.8488	7.46840	8.41097	10.9350	7.03822	6.75829	8.45811

Table 7. Maximum equivalent stress of inner tank with different parameter (unit: MPa)

A/L	B=200 mm			B=400 mm			B=600 mm		
	20 m^3	30 m^3	50 m^3	20 m^3	30 m^3	50 m^3	20 m^3	30 m^3	50 m^3
0.04	68.2549	87.3209	95.5116	62.7473	69.9898	73.8369	-	-	-
0.06	68.8506	88.3382	95.5118	56.7334	65.0059	72.0342	55.4381	62.2395	66.0393
0.08	68.5016	87.6075	98.8689	57.5003	65.5230	73.8545	51.8557	58.0805	64.2901
0.10	68.9696	83.0038	92.7951	57.2561	66.9109	72.6721	52.1278	59.1026	65.9141
0.12	68.6460	85.1315	96.4633	57.8443	65.7599	73.5615	53.0681	58.2650	65.4727
0.14	66.1417	84.2865	90.9187	56.6423	65.1615	70.4467	53.4329	58.9215	65.2010
0.16	66.9094	83.6157	92.2993	58.3434	63.7281	70.6682	53.0179	58.5512	64.3224
0.18	68.9953	82.3092	97.5639	60.8599	64.8042	73.4602	54.3998	58.4153	66.6748
0.20	70.8822	77.4839	95.4337	62.1410	67.4851	74.5926	55.9736	60.7729	69.4508
0.22	72.6903	79.4312	103.621	64.5266	68.6120	77.4575	58.2393	62.2957	69.4660

5.2 Analysis of oil tank stress distribution

The maximum equivalent stress of outer tank, middle layer and inner tank with different parameter were extracted in Tables 5, 6 and 7. It can be seen from Table 5 that the maximum equivalent stress of the outer tank increases with the increase of the support position A/L, and decreases with the increase of the bearing width B. Moreover, the maximum equivalent stress of the outer tank increases with the increase of tank volume. In Table 6, the maximum equivalent stress variation of middle layer is not obvious, but the maximum stress value is much smaller than that of the inner tank and the outer tank. It can be seen in Table 7 that the maximum equivalent stress of the inner tank decreases with the increase of the bearing width B, and increases with the increase of the tank volume. With the change of support position A/L, the variation of the maximum equivalent stress is not obvious, but it is maintained at a stable value. On the whole, the maximum equivalent stress of the inner tank is larger than that of the outer tank, and the

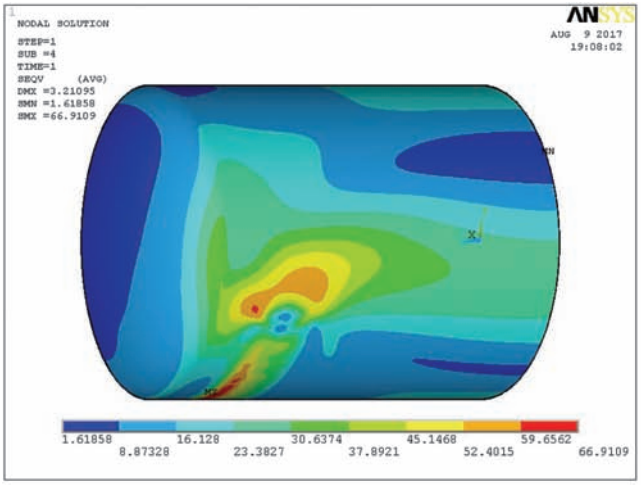

(a) Equivalent stress of internal face

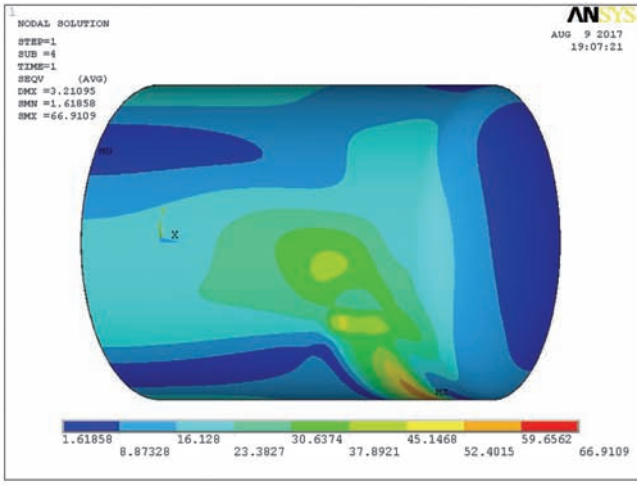

(b) Equivalent stress of outer wall surface

Fig.8. Equivalent stress of inner tank

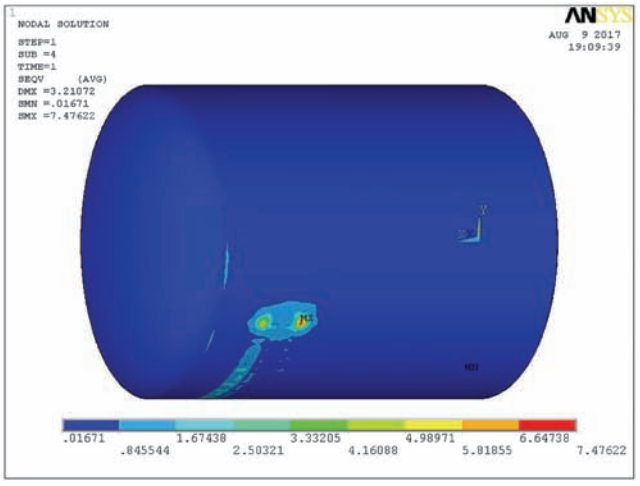

(a) Equivalent stress of internal face

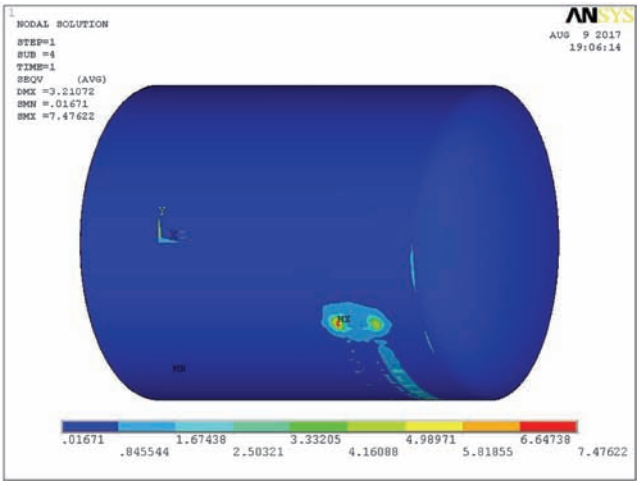

(b) Equivalent stress of outer wall surface

Fig.9. Equivalent stress of middle layer

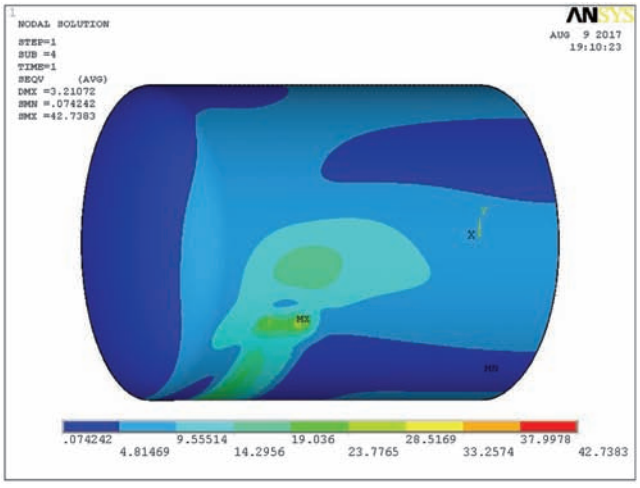

(a) Equivalent stress of internal face

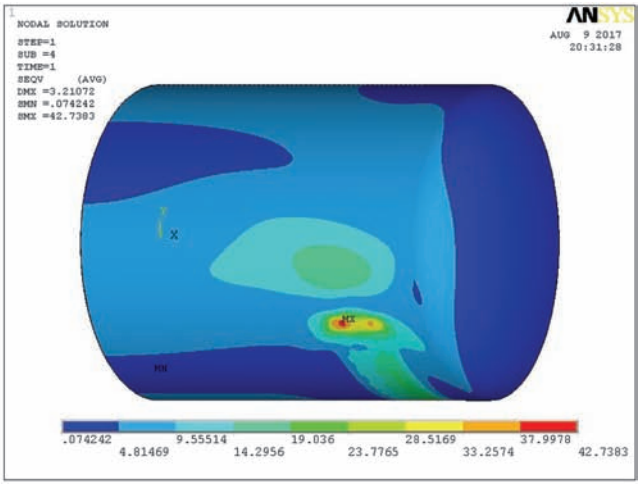

(b) Equivalent stress of outer wall surface

Fig.10. Equivalent stress of outer tank

maximum equivalent stress difference between the inner tank and outer tanks is getting smaller and smaller as the supporting position A/L increases.

Taking the model of the double-wall oil tank with the capacity of 30m^3, the supporting position A/L=0.10 and the bearing width B=400 mm as an example, the equivalent stress cloud of steel inner tank are shown in Fig.8. It can be seen from the figure that the maximum equivalent stress is 66.9109 MPa and the stress concentration in the inner tank is mainly on the outboard of the bearing and the inner wall near the sharp corners of the bearing due to the deformation curvature is large in this area. Fig.9 shows the equivalent stress cloud of middle layer. In Fig.9, the maximum equivalent stress of middle layer is almost zero except at the angular position of bearing. And, the maximum equivalent stress value is only 7.47622 MPa illustrating that the structure of the middle layer has little influence on the structural strength of the double-wall tank, and its effect is to transfer the soil load of the outer tank evenly to the inner tank. Fig.10 shows the equivalent stress cloud of outer tank. It can be seen from the figure that the equivalent stress of the outer tank is concentrated on the outer wall surface of the bearing, and the maximum equivalent stress is as high as 42.7383 MPa, pointing out that this position is the dangerous area of the outer tank.

5.3 The influence of bearing support position on stress distribution

Taking those series models of the double-wall oil tank with the capacity of 30m^3 and the bearing width B=400 mm as examples. Fig.11 shows the axial stress of intermediate section of tank. It can be seen from the figure that the axial stress variation regulation of the inner tank and the outer tank in the middle section is basically the same, but the axial stress of the steel inner tank is obviously larger than that of the FRP outer tank. Due to the influence of the soil pressure, the axial stress value of the upper ($\varphi = 180^o$) and lower ($\varphi = 0^o$) parts of the middle section of the tank is negative, but the absolute value of the axial stress in the upper part of the tank is larger than that in the lower part of the tank. What is more, the axial stress at the middle position ($\varphi = 90^o$) of the middle section of the tank is positive. With the increase of the supporting position A/L, the absolute value of the axial stress at the upper, lower and middle position of the middle section of the tank is increasing, but the magnitude of the growth of the lower part is larger than that of the upper part. The growth rate of the axial stress of the upper and lower part of the oil tank decreases with the increase of A/L, and the growth rate of axial stress at the central position of the middle section of the tank increases with the increase of A/L.

Fig.12 shows the axial stress regulation at bottom position of tank $\phi = 0°$, and Fig.13 shows the axial stress at upper position of tank $\phi = 180°$. Through the comprehensive analysis of these two figures, it is found that the bearing closer to the ellipsoid parts of oil tank, the lower the axial stress value of the tank, and the better will be the overall force of the tank. Particularly, when the bearing is located in the ellipsoid connection site of tank, the axial stress at upper and lower part of the tank are relatively small. Separately, in Fig.12, the axial stress near the bearing appears to oscillate violently in the lower part of the tank. The axial stress variation is very complicated, and the oscillation intensity of the outer tank is larger than that of the inner tank. In Fig.13, the axial stress of tank change gently in the upper part of the tank, and the axial stress reaches its maximum value at the middle section of the tank. It is shown that the stress near the bearing position is large, and the peak stress increases as the increase of bearing position A/L.

Fig.14 is a circumferential variation of the axial stress on the inner wall of the inner tank and the outer wall of the outer

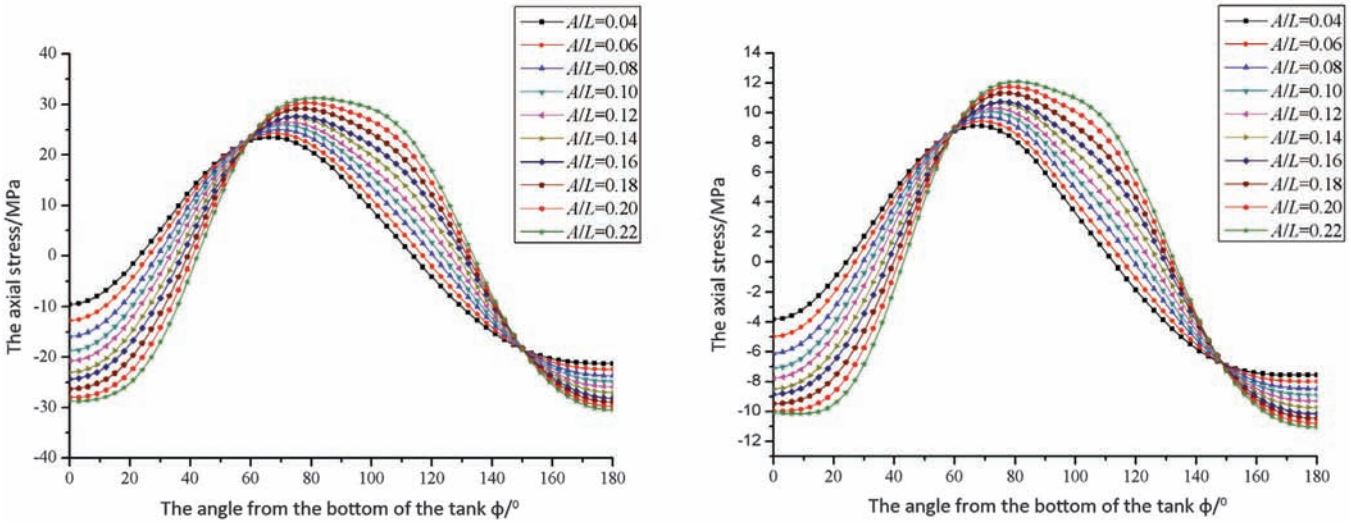

(a) inner tank (b) outer tank

Fig.11. Axial stress of intermediate section of tank

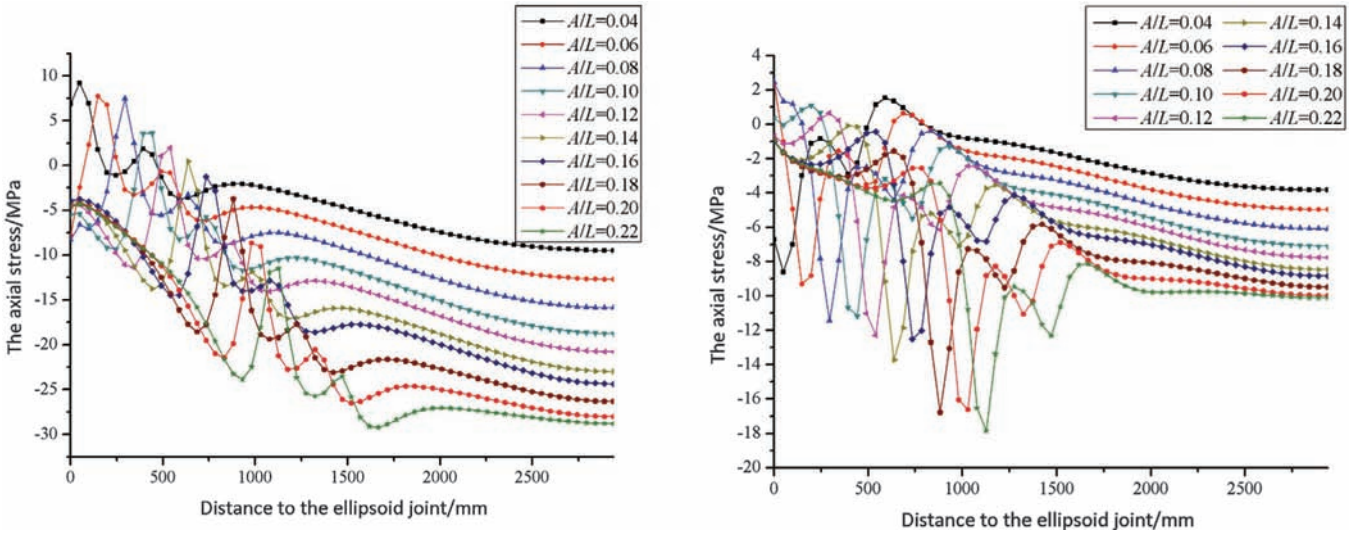

(a) inner tank (b) outer tank

Fig.12. Axial stress at bottom position of tank = 0°

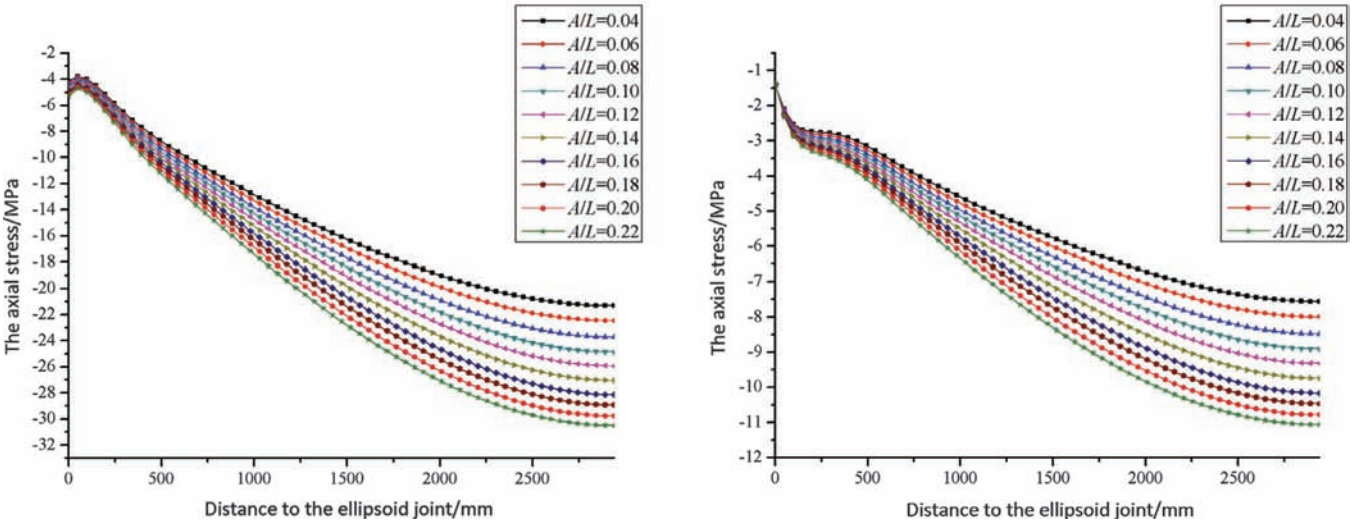

(a) inner tank (b) outer tank

Fig.13. Axial stress at top position of tank = 180°

tank at the outer edge of the support. It can be seen from the diagram that the maximum axial stress of the outer tank is about half of the maximum axial stress of the inner tank. Where the tank is in contact with the support (φ=0~60^o), the axial stress of oil tank varies gently. In the inner wall of the inner tank, the axial stress at this place is small, and as the support position A/L increases, the axial stress gradually changes from the positive to negative. While on the outer wall surface of the outer tank, the axial stress at this place is negative, and the absolute value of the axial stress is larger than that of the inner tank and increases with the increase of support position A/L. When the angle from the bottom of the tank $\varphi > 60^o$, the axial stress begins to increase rapidly and reaches the maximum value at $\varphi = 80^o$. The maximum value of the axial stress increases with the increase of the support position A/L. What is more, the axial stress began to decrease rapidly when $\varphi = 80^o$. Fig.15 is a circumferential variation of the circumferential stress on the inner wall of the inner tank and the outer wall of the outer tank at the outer edge of the support. In Fig.15, there is obvious circumferential stress concentration phenomenon near the support. In the inner tank, the stress concentration direction is positive and the circumferential stress increases with the increase of the supporting position A/L. In the outer tank, the stress concentration direction is negative and the circumferential stress decreases with the increase of support position A/L.

Fig.16 is a circumferential variation of the axial stress on the inner wall of the inner tank and the outer wall of the outer tank at the center position of the support. As can be seen from the diagram, the stress distribution regulation in this case

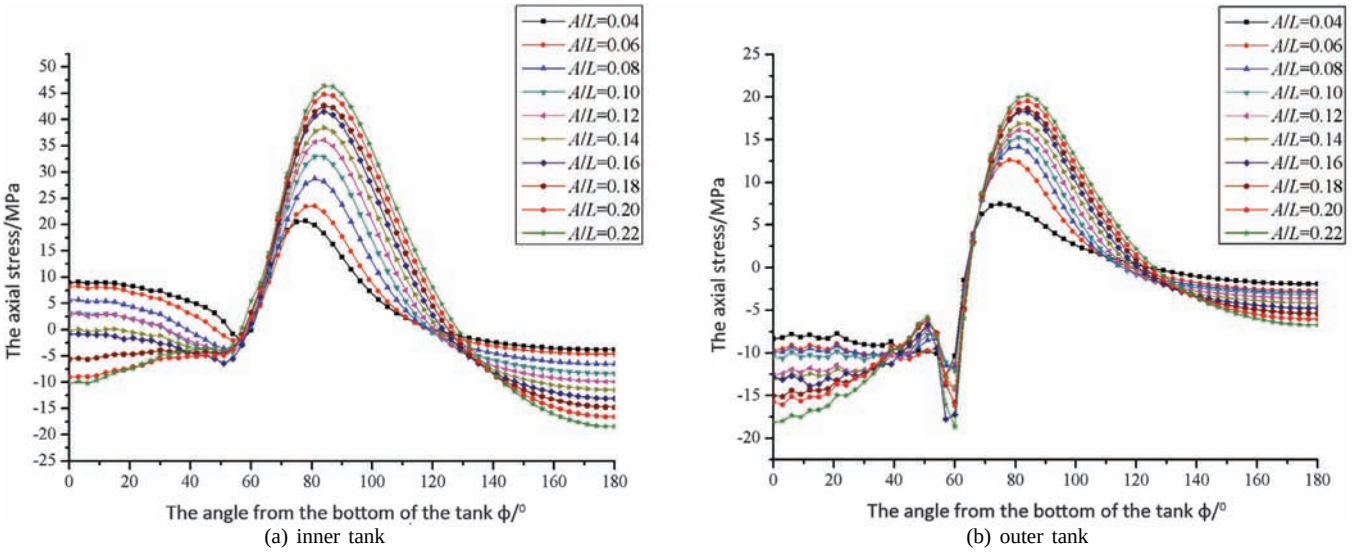

(a) inner tank (b) outer tank

Fig.14. Axial stress at outside of bearing of tank

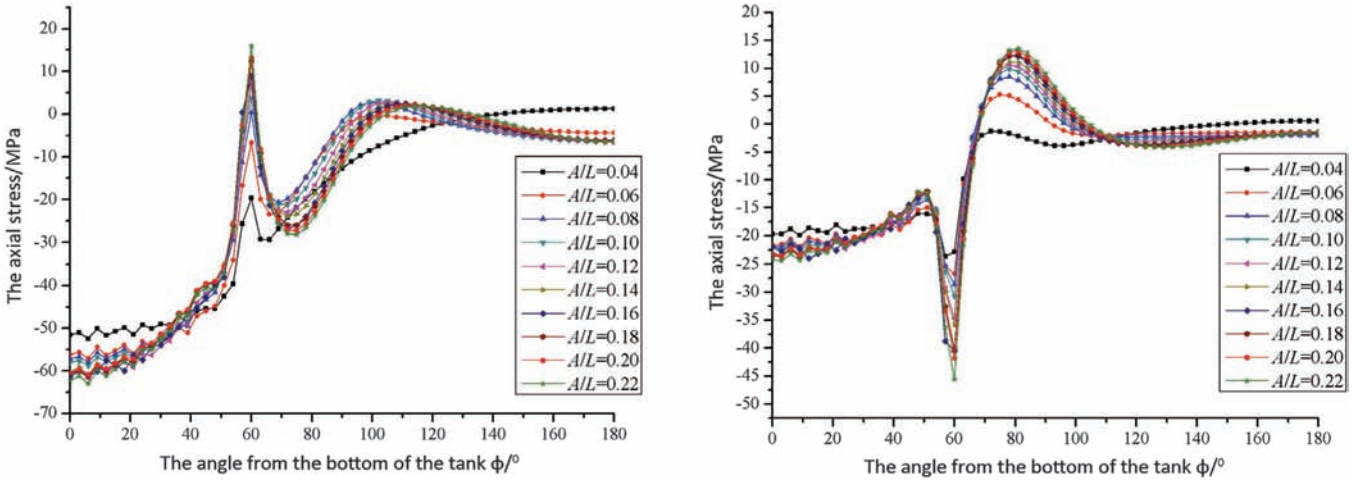

(a) inner tank (b) outer tank

Fig.15. Circumferential stress at outside of bearing of tank

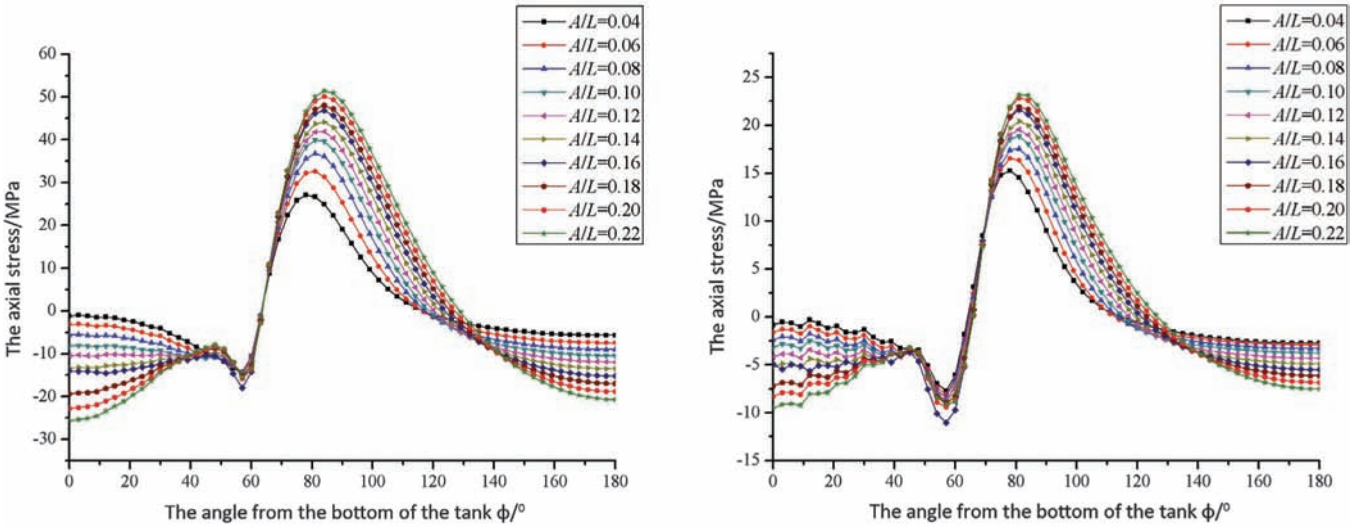

(a) inner tank (b) outer tank

Fig.16. Axial stress at middle position of bearing of tank

is similar to that of the outer edge of the support as shown in Fig.14. But at the contact point between the tank and the support, the axial stress on the inner wall of the inner tank at the center position of the support is smaller than that of the outer edge of the support, and the axial stress on the outer wall of the outer tank at the center position of the support is about the same as that of the outer edge of the support. When the angle from the bottom of the tank $\varphi = 80^{o}$, the maximum axial stress of the inner tank is larger than that of the outer edge of the support, and the maximum value of the axial stress of the outer tank is the almost the same as that of the former. Fig.17 is a circumferential variation of the circumferential stress on the inner wall of the inner tank and the outer wall of the outer tank at the center position of the support. At the contact point between the tank and the support, the absolute value of circumferential stress in the inner tank is much larger than that of the outer tank, but it is stable near a specific value. Moreover, there are obvious stress concentration areas at the corner of the support where $\varphi = 60^{o}$.

Fig.18 is a circumferential variation of the axial stress on the inner wall of the inner tank and the outer wall of the outer tank at the inner edge of the support. It can be seen from this figure that the change of axial stress in the inner tank is relatively gentle and there is no stress concentration phenomenon, while the stress concentration is obvious at the corner position of the bearing where $\varphi = 60^{o}$, and the maximum axial stress value decreases with the increase of support position A/L. Fig.19 is a circumferential variation of the circumferential stress on the inner wall of the inner tank and the outer wall of the outer tank at the inner edge of the support. In the contact area between the tank and the bearing, the circumferential stress of the inner tank decreases with the increase of A/L, and the circumferential stress of the outer

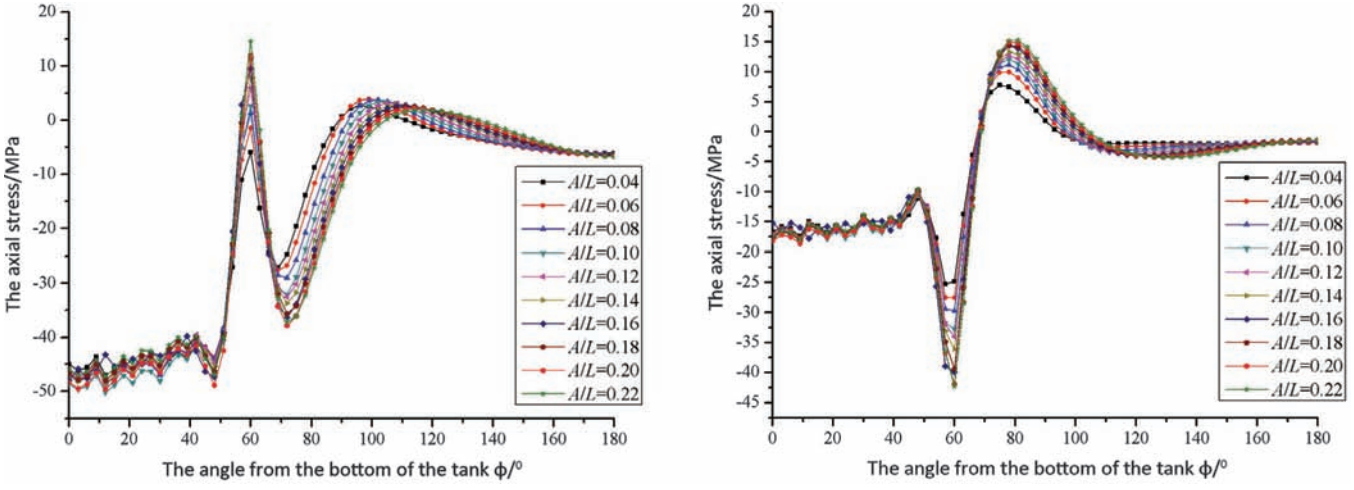

(a) inner tank (b) outer tank

Fig.17. Circumferential stress at middle position of bearing of tank

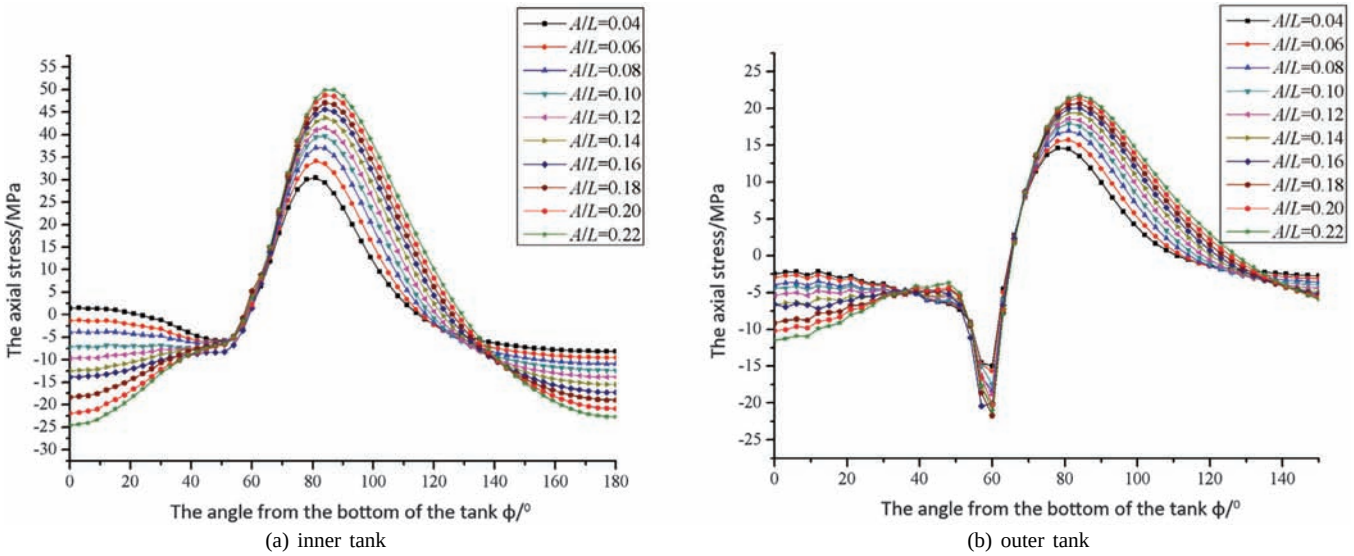

(a) inner tank (b) outer tank

Fig.18. Axial stress at inner side of bearing of tank

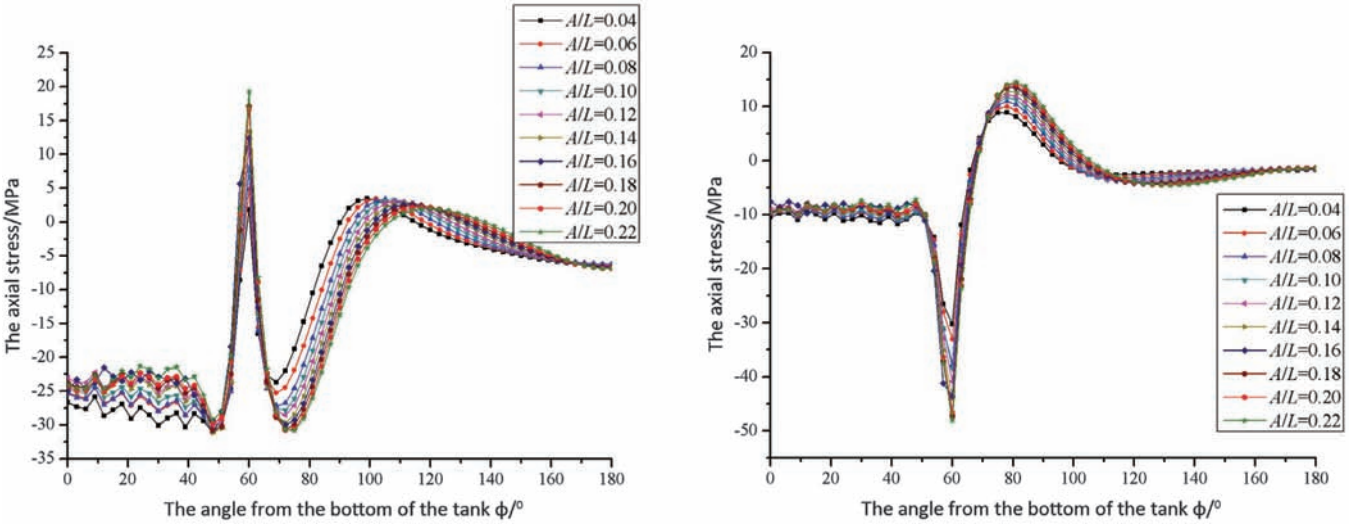

(a) inner tank (b) outer tank

Fig.19. Circumferential stress at inner side of bearing of tank

tank does not change with the change of A/L, which is basically kept at a stable value. In addition, there is a significant stress concentration in the bearing corners, and the stress is larger than that of the rest part of the bearing.

From the above analysis, it can be known that both the axial stress and circumferential stress, the stress value of inner tank is bigger than that of the outer tank. The stress distribution in the tank near the bearing is complicated. And, in the part where the tank is in contact with the bearing, the axial stress and the circumferential stress do not change with the circumferential angle, but the circumferential stress value is larger than the axial stress value. There is a significant stress concentration of the circumferential stress at the tip of the bearing, and the maximum circumferential stress changes with the change of the supporting position. Besides, at the upper part of the bearing corners, the maximum axial stress occurs, and the maximum axial stress increases with the increase of support position A/L. In addition, the stress distribution in the tank where away from the contact area between the tank and the bearing is gentle and the circumferential stress is much less than the axial stress. When the support position is closer to the ellipsoid of the tank, the overall stress distribution of the tank is better.

6. Conclusion

In this paper, the installation method of underground oil tank and the distribution of soil pressure outside the tank are analyzed. According to the structural characteristics of SF double-wall oil tank, a simplified finite element model of double tank is established. Focusing on the 20 m^3, 30 m^3 and 50 m^3 oil tanks which are widely used in the current gas stations, the deformation and stress distribution of the oil tanks under different bearing width and support position are calculated by ANSYS software respectively. Taking the 30 m^3 oil tank as an example, the deformation, stress distribution characteristics and the influence of the bearing support position on the stress distribution are analyzed in detail. The results show that:

(1) The steel inner tank of SF double tank is the main structural strength part of the tank and bear most of the load of oil tank.

(2) The maximum deformation of the tank decreases with the increase of the bearing width, and increases with the increase of the supporting position. The maximum equivalent stress of the outer tank of double-wall tank is decreased with the increase of the bearing width, and increases with the increase of the supporting position. While the maximum equivalent stress of the inner tank of double-wall tank is decreased with the increase of the bearing width, but there is no obvious correlation with the support position.

(3) The stress concentration area of the double tank is mainly distributed in the inner wall of the tank at the outer edge of the bearing, near the sharp corners of the bearing and the upper part of the bearing where $\varphi = 80^o$. And when the support position is closer to the ellipsoid of the tank, the overall stress distribution of the tank is better.

Acknowledgments

This paper is supported in part by The National Key Technology R&D Program of China (2017YFC0806306), Education Science fund of the Military Science Institute of Beijing, China (No.2016JY481), and Chongqing Graduate Scientific Research Innovation Project, China (No.CYB17148).

Reference

1. Aimikhe, V. J. Predicting critical internal diameters of onshore LNG storage tanks for minimizing boil off gas

production; proceedings of the Society of Petroleum Engineers Nigeria Annual International Conference and Exhibition 2011, August 1-3, 2011, Abuja, Nigeria, F, 2011 [C]. Society of Petroleum Engineers.

2. Arao, M., Tashima, T., Inage, K., Soma, H., Saito, S., Kawaji, S. (1998): Flexible intelligence machine control and its application to jacket tank temperature control; proceedings of the Proceedings of the 1998 IEEE International Conference on Systems, Man, and Cybernetics Part 2 (of 5), October 11-14, 1998, San Diego, CA, USA, F, [C]. IEEE.
3. Bridges, T. F. (1971): Features of a double- wall, self-supporting tank system for LNG. Shipbuilding & Shipping Record, 117(5-6): 59, 61-59, 61.
4. GB 50156-2012: Code for design and construction of filling station[S].
5. GB 50074-2014: Code for design of oil depot[S].
6. He, M., Liang, Z., Li, Y. (2007): Design and research of underground oil tank. *Petro-Chemical Equipment Technology*, 28(06): 14-16.
7. Jeong, J.-H., Choi, D.-J., Won, J.-P., Park, D.-H., Lee, S.-Y., Lee, M.-H., Kim, Y.-H., Moon, K.-M. (2013): Evaluation of thermal conductivity and heat flux by insulation analysis of double-wall for cryogenic storage tank; proceedings of the 3rd International Conference on Advanced Engineering Materials and Technology, AEMT 2013, May 11-12, 2013, Zhangjiajie, China, F, 2013 [C]. Trans Tech Publications Ltd.
8. Kaempen, C. E. (1996): Steel-stiffened filament-wound double-wall fiberglass composite underground storage tanks. International SAMPE Symposium and Exhibition (Proceedings), 41(2): 1655-1666.
9. Li, Y., Liu, Q., Meng, H., Sun, L., Zhang, Y.(2013): The electrostatic properties of Fiber-Reinforced-Plastics double wall underground storage gasoline tanks; proceedings of the 7th International Conference on Applied Electrostatics, ICAES 2012, September 17-19, 2012, Dalian, China, F, 2013 [C]. Institute of Physics Publishing.
10. Liu, Y., Liu, W. S., Nan, Y., Zhang, T., University, S. (2015): Finite Element analysis of FRP Buried Double-wall Oil Sstorage Tank. Fiber Reinforced Plastics/ composites, 15(4): 1390-1411.
11. Mjalli, F. S., Jayakumar, N. S. (2009): An Algorithm for Stabilizing Unstable Steady States for Jacketed Nonisothermal Continually Stirred Tank Reactors. Industrial & Engineering Chemistry Research, 48(16): 7631-7636.
12. Song, J. (2002): Design of buried oil tank. Petroleum Engineering Construction, 28(3): 4-7.
13. Tan, J. (2002): Finite element analysis based on ANSYS 6.0[M]. Beijing: Peking University Press.
14. DB 11/588-2008. Technical code for prevent leakage of underground storage tank [S].
15. Wang, W., Gao, D. Double layer oil storage tank and manufacturing method: China, 201210190033.8 [P]. 2012-9-26.
16. Wilkowski, G., Shim, D.-J., Brust, B., Rana, M. D. (2010): Failure investigation of a 500 gallon liquid nitrogen storage tank; proceedings of the ASME 2010 Pressure Vessels and Piping Division/K-PVP Conference, PVP2010, July 18-22, 2010, Bellevue, WA, United states, F, 2010 [C]. American Society of Mechanical Engineers.
17. Wu, Y.-L., Wang, D.-C., Zhou, H.-Q. (2002): Design and fabrication of large welded steel double-wall refrigerated tank. Shiyou Huagong Shebei/Petro-Chemical Equipment, 31(1): 39-39.
18. Yang, J., Wang, H. E., Mingzhong, D. U., Zhang, F. (2016): The Application Prospect of Double-Deck Oil Tank in China. *Journal of Chongqing University of Science & Technology*.
19. Yang, (2000): Q.Micromechanics and design of composite materials[M]. BeiJing: China Railway Press.
20. Zhou, W., Zhang, Q., Chen, H. (2007): Design and Calculation of Horizontal Vessel Buried Beneath Driveway. Process Equipment & Piping, 44(1): 16-17.